An Experiment to Search for Neutrino Oscillations Using a ν_e Enriched Beam

U. Camerini, C. Canada, D. Cline, G. Bauer, W. Fry, R. Loveless, J. Matthews, R. Morse, M. Mohammadi, A. More, D.D. Reeder A. Szentgyorgi, H. Wachsmuth
University of Wisconsin, Madison, Wisconsin

C. Kourkoumelis, A. Markou, L.K. Resvanis
University of Athens, Athens, Greece

R. Huson, D. Ljung, J. Schmidt, W. Smart, R. Stefanski, E. Treadwell
Fermilab, Batavia, Illinois

M. Baldo-Ceolin, F. Bobisut, E. Calimani, G. Puglierin, A. Sconza
Instituto di Fisica, Universita di Padova, Padova, Italy*

*Universita di Padova's participation is subject to Italian authorities' approval.

I. An Experiment to Search for Neutrino Oscillations Using a ν_e Enriched Beam

Athens-Fermilab-Padova-Wisconsin Collaboration

It is proposed to search for electron neutrino oscillations using a ν_e enriched beam and the 15' bubble chamber filled with a heavy neon-hydrogen mixture.

The sensitivity of the experiment can be expressed in several ways depending on the signal used:

1) $P(\nu_e \to \nu_\tau) \gtrsim$ 1-2%. This is achieved by the direct observation of the ν_τ by kinematical consideration of the charged current interactions and by detection of the visible decay.

2) $P(\nu_e \to \nu_e) \gtrsim 0.9$. This is achieved by the observation of an anomalous ratio of e/μ charged current interactions or an anomalous ratio of neutral current to charged current events.

3) In the context of two neutrino oscillations the limits of the difference in mass squared (Δ) and the mixing angle ($\sin^2 2\theta$) are: $\Delta \gtrsim 5(\mathrm{eV})^2$ and $\sin^2 2\theta \gtrsim .05$.

About 330,000 pictures are required which would be $\lesssim$ 10 weeks of accelerator time in a dedicated mode. This would result in 10^{19} protons on target and would yield the necessary 1000 ν_e charged current interactions.

II. Introduction

The possible existence of differing types of massive neutrinos and oscillatons between them remains a question of great interest.[1] If this phenomenon is established, it will significantly affect not only the physics of elementary particles, but also astrophysics and cosmology. At the time of submission of P-655 we noted several new phenomenological analyses of the existing data.[2,3,4] A conclusion of this work was that the possibility exists that oscillations occur which have shorter wavelengths than previously considered. The most definitive positive experimental observation is that of Reines et al.[5] They have responded to questions and criticisms and the experiment still appears to suggest that the probability of ν_e to remain ν_e is significantly less than one. Similarly, one explanation of the recent results on the lack of solar neutrinos reported by Davis et al.,[6] and the comparison to solar ν flux calculations by Bahcall et al.,[7] is neutrino oscillations. Although oscillations alone may not entirely explain the anomaly.

A sine qua non for neutrino oscillations is that neutrinos are massive. A Moscow experiment to measure the end point of the tritium β-decay spectrum has reported a neutrino mass m_ν in the range 14-46 eV.[8] Another interesting speculation consistent with the lower values of this range was made by F. Stecker.[9] He suggests that one explanation of a "line" observed in UV astronomy is that it arises from the decay of galactic halo neutrinos.

Two types of neutrino oscillations have been suggested[3]

a) First kind $\nu_\mu \rightleftarrows \nu_e$, $\nu_\mu \rightleftarrows \nu_\tau$, $\nu_e \rightleftarrows \nu_\tau$

b) Second kind $\nu_{\mu L} \rightleftarrows \eta_{\mu L}$, $\nu_{eL} \rightleftarrows \eta_{eL}$, $\nu_\tau \rightleftarrows \eta_{\tau L}$

where η is a left-handed singlet.

The signal for the first kind of oscillation would be the disappearance of one kind of neutrino and its reappearance as another kind. This change of type would be detectable only by charged current interactions, neutral current interactions would be unchanged. For oscillations of the second kind neutrinos would disappear with no subsequent interaction of the new neutrino.

If we consider only oscillations between two types the probability for $\nu_\alpha \rightarrow \nu_\beta$ can be written

$$P(\nu_\alpha \rightarrow \nu_\beta) = \delta_{\alpha\beta} - \sin^2 2\theta \, \sin^2(1.27\frac{\Delta L}{E})$$

where

$\Delta = m_\alpha^2 - m_\beta^2$ $(\mathrm{eV})^2$ difference in mass squared of the two neutrinos

L = (meters) path length of neutrino

E = (MeV) energy of the neutrino

$\sin^2 2\theta$ = the mixing angle between the two neutrinos

Oscillations between three neutrino types lead to a more complicated equation involving another mixing angle. This is needlessly complicated in view of the experimental limits on ν_μ oscillation.

The experimental situation is shown in Figure 1 in which the probability is plotted against L/E. The possible oscillation of ν_μ is severely restricted by existing experiments. However, the limits on ν_e are much less restrictive. We note that the positive experimental indications all involve ν_e not ν_μ.[5,6,8]

Another way of displaying the experimental results is to plot the allowed and forbidden values of Δ and $\sin^2 2\theta$. As an example we show the limit obtained in the Los Alamos experiment[10] *in Figure 2*. The effect of averaging over the energy spectrum is clearly seen. The curve shown is obtained by averaging the result for $P(\nu_e \rightarrow \nu_e) = 1.09\pm^{.37}_{.41}$ at the 1σ level with the observed spectrum. This figure illustrates that not only the mean L/E but also the range of L/E is important in order that an experiment completely restrict the possible values of Δ and $\sin^2 2\theta$.

III. Physics Goals

We propose to search for oscillations of the electron neutrino by using a neutrino beam with a large fraction ($\sim$ 50%) of electron neutrinos. The 15' FNAL Bubble Chamber filled with 70% neon in hydrogen is used as the target and detector. The signals of oscillations would be:

a) $P(\nu_e \rightarrow \nu_\tau)$ The identity of the final state τ neutrino is determined by the charged current interaction. Because of kinematic suppression of the charged current cross section, the direct detection of the τ neutrino is possible only for $E_\nu \gtrsim 10$ GeV. The 15' neon bubble chamber is an ideal instrument for the detection of the τ lepton. Furthermore, the use of the bubble chamber enables us to discern the τ decay vertex for a fraction of the τ's produced.

b) $P(\nu_e \rightarrow \nu_e)$ The excellent capability of the bubble chamber to detect electrons can be used to:

- measure the ratio of electron to muon charged current events $R(e/\mu)$. An anomalous value of R could indicate oscillations of both the first and second kinds.
- separate neutral current events from charged current interactions $R(N_\circ/N_\ell)$. This ratio would be sensitive only to oscillations of the first kind.

IV. Beam Description

Previous accelerator experiments have been insensitive to ν_e oscillations because of small ν_e flux and/or a very large accompanying ν_μ flux. We propose to construct a $\nu_e/\bar{\nu}_e$ beam with a ν_e/ν_μ ratio close to unity. A beam with this feature has been previously designed.[11,12] Figure 3 schematically shows the beam arrangement. The Sign Selected Bare Target (SSBT) train used for the HPWF neutrino experiment could be modified for this electron neutrino beam. The principal idea is to sweep all charged particles out of the beam using a dipole placed just downstream of the target. A second dipole located farther downstream, sweeps out the charged decay products from K_S° decays. Electron neutrinos are produced from $K_L^\circ \rightarrow \pi^- e^+ \nu_e$ (or $\rightarrow \pi^+ e^- \bar{\nu}_e$) decay. Figure 4 shows a Monte Carlo calculation of the neutrino fluxes in a beam using 400 GeV incident protons. The neutral kaon production is assumed to be the average of K^+ and K^- production. The muon neutrino background from $K_{\mu 3}^\circ$ decay and π and K decays is also shown. Note that above about 20 GeV the electron neutrino flux is nearly equal to the muon neutrino flux.

V. Detector and Event Rates

The 15' bubble chamber and the two-plane EMI form an excellent detector for neutrino events. The use of the heavy liquid bubble chamber has the following well-known advantages:

1) excellent identification of electrons ($\sim$ 95%) and muons ($\sim$ 80%) with both sign and momentum determination and $\sim$ 80% γ detection.

2) good efficiency for observing and measuring complicated exclusive channels.

3) excellent visibility of the vertex. It would be possible to see the τ lepton decay vertex depending on the τ momentum spectrum and lifetime. The addition of a high resolution camera to the stereo triad would considerably enhance this possibility.

4) unbiassed data taking. The detection of events and energy resolution are independent of the kinematic characteristics and/or the event energy, which allows the experiment to cover a wide range of L/E.

We propose a heavy mix of neon in hydrogen to optimize event rates. As a goal we wish to obtain 1000 ν_e charged current interactions in order to be sensitive to $P(\nu_e \rightarrow \nu_\tau) \sim$ 1-2%. This requires approximately 10^{19} protons on target at 400 GeV. The numbers of neutrino events of the various types in two momentum intervals are shown in Table I. The number of ν_τ entered in Table I is calculated from the decay of charmed particles produced in the target and is the background to the oscillation signal.

The time required for such an exposure is of concern in these days of limited accelerator utilization. The efficiency of the exposure is maximized if the entire beam intensity is used. The number of bubble chamber pictures is minimized and the total time to achieve 10^{19} p.o.t. is minimized. In this dedicated running mode power consumption is significantly reduced compared to conventional running. Not only are there no secondary beam lines energized (except the train), no flat top on the accelerator field is needed. The latter feature reduces power required even with an increased repetition rate.

The running time needed for the 330,000 picture exposure is about 10 weeks assuming the proven ability of the accelerator to deliver 10^{18} p.o.t. per week.

TABLE 1

Event rates

expected for 15 ton and 10^{19} protons on 1 λ_{abs} target

	CC[a]			NC[b]			e/μ ratio		
	10-40	>40	total	10-40	>40	total	10-40	>40	total
ν_e	150	870	1020	45	260	305			
$\bar{\nu}_e$	75	420	495	25	143	168			
ν_μ	240	960	1200	72	288	360	.63	.91	.85
$\bar{\nu}_\mu$	125	330	455	43	112	155	.60	1.25	1.09
ν_τ[c]			<4						

(a). From spectra in fig. 3 assuming $\sigma^{\nu} = 0.62E \times 10^{-38}$, $\sigma^{\bar{\nu}}/\sigma^{\nu} = 0.48$. 75 prompt ν_e, ν_μ (36 $\bar{\nu}_e$, $\bar{\nu}_\mu$) events are included (CERN beam dump result).

(b). NC/CC = 0.30 for ν, 0.34 for $\bar{\nu}$.

(c). Assumes $F\bar{F}/D\bar{D} = 0.1$, BR($F \to \tau\nu$) = 0.03.

VI. Details of the τ Search

a) Kinematic Analysis

We propose to identify the presence of ν_τ and $\bar{\nu}_\tau$ through the characteristic τ decay signatures. These decays can be grouped into two general categories (shown in Figure 5) according to the type of background that must be eliminated. Decays of the type illustrated in Figure 5 appear as somewhat unusual charged current electron events with missing neutrinos. The other type resemble neutral currents in that they have no charged e or μ lepton, only a missing neutrino. Table 2 shows a summary of the τ decay modes, the estimated efficiency, and the ultimate sensitivity of each channel. In this calculation we have included τ threshold effects which reduce the cross section for ν_τ CC interactions relative to ν_μ CC *interactions* by 22% (Figure 6) averaged over our neutrino spectrum.[13]

Table 2

τ Decay Mode	Branching Ratio	Detection Efficiency	Background Fraction	Sensitivity (Minimum Value $P(\nu_e \to \nu_\tau)$ Detectable)
1. $e\nu\bar{\nu}$	17%	10.7%	0.3% of ν_eCC	∿ 20%
2. $\mu\nu\bar{\nu}$	17%	8.7%	0.3% of ν_μCC	∿ 20%
3. $\pi\nu$	9%	30.0%	0.3% of NC	14%
4. $\rho\nu$	22%	∿ 50.0%	0.05% of NC	1.5%
5. $\pi\rho^\circ\nu$	4%	∿ 50.0%	0.1% of NC	6%
6. $n\pi\nu$	31%	∿ 50.0%	2.0% of NC	17%

We discuss each of these channels in detail below.

b) Leptonic Decays (decays 1 and 2)

As shown schematically in Figure 5b the missing neutrinos typically have a large transverse momentum ($p_\perp$) directed oppositely to the hadronic transverse momentum. Three independent variables which can be used to distinguish a τ decay from an ordinary CC event are: the missing transverse momentum ($p_\perp^\circ$); the angle (ϕ) between the lepton transverse momentum and the $p_\perp^\circ$; and the longitudinal momentum of the lepton (P_L). Generally, we follow the analysis discussed by Albright et al.[14] although we include additional information from the lepton longitudinal momentum to achieve better background rejection.

To estimate the background we use a sample of 1500 CC events (average energy $\sim$ 30 GeV) from Exp. 28.[15] These events were a portion of an ν exposure of the 15' BC (20% neon) with 300 GeV protons and horn focussing. They are representative of the energy, complexity, and resolution of the event sample expected from the K_L° beam. In Figure 7a we plot $p_\perp^\circ$ vs. ϕ for 1440 ν_μ events. With the selection region as indicated by the dotted lines 0.3% of the conventional charged current interactions are accepted.

In Figure 7b we show the same distribution for τ leptons. The τ events were simulated by assuming each of the muons in the CC sample was a τ and then calculating the τ decay to $e\nu\bar{\nu}$ by Monte Carlo. With the same cuts as for the conventional events about 11% of the τ are accepted. This analysis realistically portrays the difficulties in separating ν_τ events and contains no assumptions concerning the effects of resolution, missing hadronic energy, etc. By enlarging the cut boundaries we can increase the τ acceptance efficiency at the expense of increasing background.

c) Hadronic Decays

i) $\tau \rightarrow \pi\nu$ (decay 3)

This τ decay produces one charged track with large transverse momentum with respect to the other hadrons (P_{th}). Three independent variables can be used to distinguish $\tau \rightarrow \pi\nu$ events: the transverse momentum of π, the longitudinal momentum of π, and the angle (θ) between the π transverse momentum $p_\perp$ and the missing $p_\perp^\circ$. To estimate the background we again use the same E-28 data sample and assume the muon to be a τ and calculate the $\pi\nu$ decay.

In the plane transverse to the neutrino direction we determine the transverse axis (TA) of the event as that direction which minimizes the orthogonal transverse momentum (similar to the thrust analysis in e^+e^- collisions). The component of the transverse momentum, $p_\perp$, of each track along this axis is plotted vs. the longitudinal momentum, as shown in Figure 9. From E-28 data we estimate a background to $\tau \rightarrow \pi\nu$ of 0.3% of NC events. The τ detection efficiency for these cuts is 30% (see Figure 9). Since the total NC sample is expected to be 1,000 events we anticipate three background events. If we detect six events (three background, three real $\tau \rightarrow \pi\nu$ decays) this channel is sensitive to $P(\nu_e \rightarrow \nu_\tau) \sim 14\%$.

ii) $\tau \rightarrow \rho\nu_\tau$ (decay 4)

For this mode the τ decay results in one charged track and two γ's. We expect to see both γ's $\sim$ 60% of the time. These tracks can be fitted to a $\rho^\pm$, which will then have a large P_{th}. Our ability to measure the γ energy (see Figure 8) allows us good resolution of the ρ mass. Since we choose events in which the angle between the hadrons and the π° (also γ's) is large, we anticipate few problems with multiple γ pairings.

By the same method used for the $\pi\nu$ decay and with a fitted ρ at large p_{th}, we estimate less than .05% of NC interactions will mimick a τ. So the observation of a single $\tau \to \rho\nu$ event (detection eff. $\sim$ .50, BR = .22) implies 10 ν_τ interactions. If there were originally 1000 ν_e, we are sensitive to a value of 1-2% for $P(\nu_e \to \nu_\tau)$. This is the most sensitive channel and sets the experimental limit.

The major reason for the decreased background in the decay is that the ρ^- multiplicity is < 0.4 per neutrino event, where as the π^- multiplicity is about three. This fact coupled with the largest branching ratio makes the $\tau^- \to \rho^-\nu_\tau$ mode by far the cleanest experimentally. We note that this procedure cannot be used by most counter experiments, particularly those utilizing hadronic calorimeters.

iii) $\tau \to \pi$'s (decays 5 and 6)

These decay channels are similar to $\pi\nu$ if the pions from the decay can be separated from the hadrons. The "thrust" analysis can be used to identify candidates which can be fitted to $A_1 \to \pi\rho$, $\pi\pi\pi$. We estimate the sensitivity of these channels to be $P(\nu_e \to \nu_\tau) \sim 17\%$.

VII. Visible Decay

The expected lifetime of the τ lepton is 2.8×10^{-13} sec., assuming full V-A coupling. Therefore, with the conventional optical system of the 15' bubble chamber we expect to see the decay vertex in 5-10% of the τ decays. Although the decays are predominately one-pronged which makes identification more difficult, this is partly compensated by the separation of the lepton from the hadron shower. We base our estimate on our experience in E-546 in which we identified more than four examples of charmed particle decay.[16]

A single high resolution camera operated in conjunction with the conventional triad would improve our resolution significantly over about one-half the fiducial volume. Subject to availability and operating cost considerations, we propose to utilize this high resolution camera.

In summary, the limits on the values of Δ and $\sin^2 2\theta$ achieved by measurement of the τ neutrinos in this experiment are shown in Figure 10. In the region above and to the right of the line, are the values which will be detected for eliminated by the experimental results. The lines are labeled by the number of τ's interacting in the bubble chamber via the charged current interaction or, alternatively, the τ detection efficiency for which 2.5 τ's are identified.

VIII. Ratio of Electron to Muon Events

Two different oscillation phenomena lead to an observed e/μ ratio which differs from the value expected from the beam fluxes. In Table I we list the calculated values of $R(e/\mu)$ in two momentum intervals.

a) $\nu_e \to \nu_\tau$, Oscillations of the first kind

In this case the ratio becomes

$$R(\frac{e}{\mu}) = \frac{\phi[1-P]\sigma_{cc} + 0.17\ \phi\ P\sigma^{\tau}_{cc}}{\sigma^{\mu}_{cc} + 0.17\ \phi\ P\sigma^{\tau}_{cc}} = \frac{[(1-P)\sigma^{e}_{cc} + 0.17\ P\sigma^{\tau}_{cc}]\phi}{\sigma^{\mu}_{cc} + 0.17\ P\sigma^{\tau}_{cc}\ \phi}$$

where $P = P(\nu_e \to \nu_\tau)$ the probability of the ν_e oscillating into ν_τ, σ^{μ}_{cc} (σ^{e}_{cc}) is the cross section for ν_μ and (ν_e), $\sigma_{cc}{}^{\tau}$ is the corresponding cross section for ν_τ interactions, and ϕ is the ratio of the ν_e flux to the ν_μ flux. For example if $P = .3$, and σ^{τ}_{cc} for our spectrum is $0.78\ \sigma^{e}_{cc}$, then R becomes

$$R(\frac{e}{\mu}) = \frac{.7\ \phi + .17(.78)\phi}{P + .17(.78)\phi} \cong .74\ \phi$$

to be compared with $R(\frac{e}{\mu}) = \phi$ for no oscillation.

b) $\nu_{eL} \to \bar{\nu}_{eL}$, Oscillations of the second kind

For this case the V-A theory predicts that the $\bar{\nu}_{eL}$ will not interact. Hence $R(\frac{e}{\mu})$ becomes

$$R(\frac{e}{\mu}) = \frac{(1-P)\sigma^{e}_{cc}\phi}{\sigma^{\mu}_{cc}} \sim (1-P)\phi$$

where now $P = P(\nu_{eL} \to \bar{\nu}_{eL})$

As in the previous example, for P = .3, $R(\frac{e}{\mu})$ becomes 0.7 ϕ, similar to the previous ratio. However, the two phenomena would be distinguished by the direct observation or non-observation of the ν_τ interaction.

The experimental significance of this ratio depends strongly on the knowledge of ϕ. From particle production data and beam geometry we believe ϕ can be determined to 5%. If this can be achieved, the measurement of $R(\frac{e}{\mu})$ would be sensitive to a value of $P(\nu_{eL} \rightarrow \bar{\nu}_{eL}) \simeq 10\%$. In Figure 11 we summarize the limits on the values of Δ and $\sin^2 2\theta$ to the experimental precision of the measurement of $R(\frac{e}{\mu})$. In the region above and to the right of the line is the range of values which can be detected or eliminated in this experiment with the fractional error shown.

IX. Ratio of Events Without and With Charged Leptons $R(N_\circ/N_\ell)$

The ratio of events without ($N_\circ$) and with (N_ℓ) a charged lepton is also sensitive to $\nu_e \to \nu_\tau$ oscillations. We define the quantities:

R	the ratio of neutral to charged current interactions
R_τ	neutral to charged ratio for ν_τ interactions ($\sim$.38 corrected for the threshold effect)
$\sigma^\mu_{cc}(\sigma^e_{cc})$	CC cross section for ν_μ (ν_e)
ϕ	ratio of ν_e flux to ν_μ flux

a) $\nu_e \to \nu_\tau$, Oscillations of the first kind

The ratio $R(N_\circ/N_\ell)$ can be calculated by summing contributions:

$$R(N_\circ/N_\ell) = \frac{\sigma^\mu_{cc}R + \phi\sigma^e_{cc}\,R(1-P) + .66\,\phi\,P\,\sigma^\tau_{cc} + \phi\sigma^\tau_{cc}R_\tau P}{\sigma^\mu_{cc} + \phi\,\sigma^e_{cc}(1-P) + .34\,\phi\,\sigma^\tau_{cc}\,P}$$

where $P = P(\nu_e \to \nu_\tau)$

Without oscillation, the ratio $R(N_\circ/N_\ell) = 0.3$, independent of the flux ratio, ϕ. However, if $P = .3$ and $\phi = 1$

$R(N_\circ/N_\ell) = (1 + \frac{5}{4}P)R_\mu = 0.42$

If $\phi << 1$ then

$R(N_\circ/N_\ell) = (1 + \frac{5}{2}\phi P)R$

illustrating the difficulty of using the neutral current signal if the ν_e flux << ν_μ flux.

Assuming ϕ we can solve for P as a function of the measured ratio, $R(N_\circ/N_\ell)$

$$P = \frac{4}{5}\left(\frac{R(N_\circ/N_\ell)-R}{R}\right)$$

For a measured $R(N_\circ/N_\ell) = 0.40\pm.02$ we can measure $\frac{\delta P}{P} \sim .20$. We note that if the measured ratio $R(N_\circ/N_\ell)$ deviates from that measured in a ν_μ beam, and, if no ν_τ CC interactions are observed, then μ-e universality is violated in the NC sector.

b) $\nu_e \to \bar{\nu}_{eL}$ Oscillations of the second kind

In this case the ratio becomes

$$R(N_\circ/N_\ell) = \frac{\sigma^\mu_{cc} R + \phi\, \sigma^e_{cc} R\,(1-P)}{\sigma^\mu_{cc} + \phi\, \sigma^e_{cc}\,(1-P)} \simeq R$$

which is independent of $P(\nu_{eL} \to \bar{\nu}_{eL})$. Hence this ratio can never be used to observe an oscillation into a neutrino which does not interact. In Figure 12 we summarize the limits on the values of Δ and $\sin^2 2\theta$ to the precision of the experimental measurement of $R(N_\circ/N_\ell)$. In the region above and to the right of the line is the range of values which can be detected or eliminated in this experiment with the fractional error shown.

REFERENCES

1. B. Pontecorvo, Soviet Phys. JETP 53, 1717 (1967); V. Gribov and B. Pontecorvo, Phys. Lett. 28B, 493 (1969).
   For thorough recent review of theory and experiment see (a) S.M. Bilenky and B. Pontecorvo, Phys. Reports 41, 225 (1978); (b) A. de Rujula et al., CERN TH-2788 (1979).
2. V. Barger et al., Physics Letters 93B 194 (1980).
3. V. Barger et al., Phys. Rev. Letters 45, 692 (1980).
4. V. Barger et al., University of Wisconsin Reports No. COO-881-135, COO-881-146, and COO-881-148 (unpublished).
5. F. Reines et al., contributed paper to the XXth International Conference on High Energy Physics, Madison, Wisconsin, July, 1980.
   F. Reines, Unification of Elementary Forces and Gauge Theories (eds. D.B. Cline and F.E. Mills), Harwood Academic Publishers, p. 103 (1978).
6. R. Davis Jr., BNL Report No. BNL 50879, 1978 Vol. 1, p. 1.
   R. Davis, Jr., J.C. Evans and B.T. Cleveland, Proc. of the Conf. on Neutrino Physics, ed. by E.C. Fowler (Purdue Univ. Press, 1978).
7. J. Bahcall et al., Phys. Rev. Letters 45, 945 (1980).
8. V. Lyubinov et al., ITEP preprint number 62, Institute of Theoretical and Experimental Physics, Moscow 1980.

REFERENCES (continued)

9. F.W. Stecker, Laboratory for High Energy Astrophysics, NASA/Goddard Space Flight Center, Greenbelt, MD 20771, preprint.

10. S. Willis et. al., Phys. Rev. Letters 44, 522 (1980) and P. Nemethy et. al., (same group) preprint.

11. D. Treille, R. Turlay, K. Winter, CERN/ECFA/72/4, Vol. 1 (1972) p. 167.

12. S. Mori, S. Pruss, and R. Stefanski, TM-725 (April, 1977). S. Mori, "Improved Electron Neutrino Beam:, TM-769.

13. K. Bonnardt, "Lepton Mass Effects in Production of Heavy Leptons by Neutrinos in Deep Inelastic Processes", Karlsruhe Preprint, TKP/9-5 (1979).

14. C. Albright, R. Shrock, and J. Smith, Phys. Rev. D20, 2177 (1979).

15. P. Bosetti, et. al., Phys. Rev. Letters 38, 1248 (1977).

16. H.C. Ballagh et. al., Physics Letters 89B, 423 (1980).

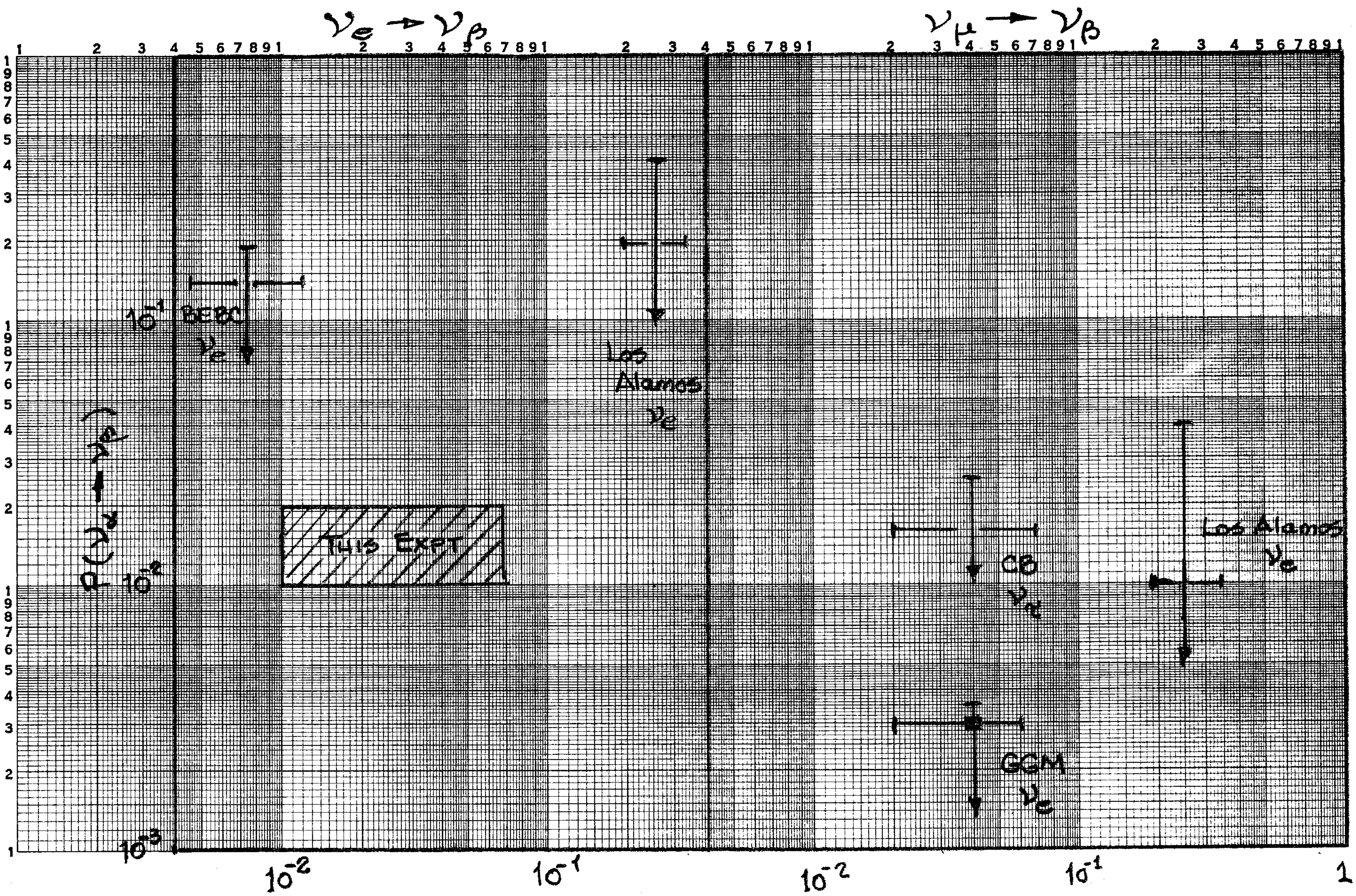

$\nu_e \to \nu_\beta$
$\nu_\mu \to \nu_\beta$
$P(\nu_\alpha \to \nu_\beta)$
10^{-1}
10^{-2}
10^{-3}
BEBC ν_e
THIS EXPT
Los Alamos ν_e
CB ν_μ
GGM ν_e
Los Alamos ν_e
10^{-2}
10^{-1}
10^{-2}
10^{-1}
1

Fig 1.

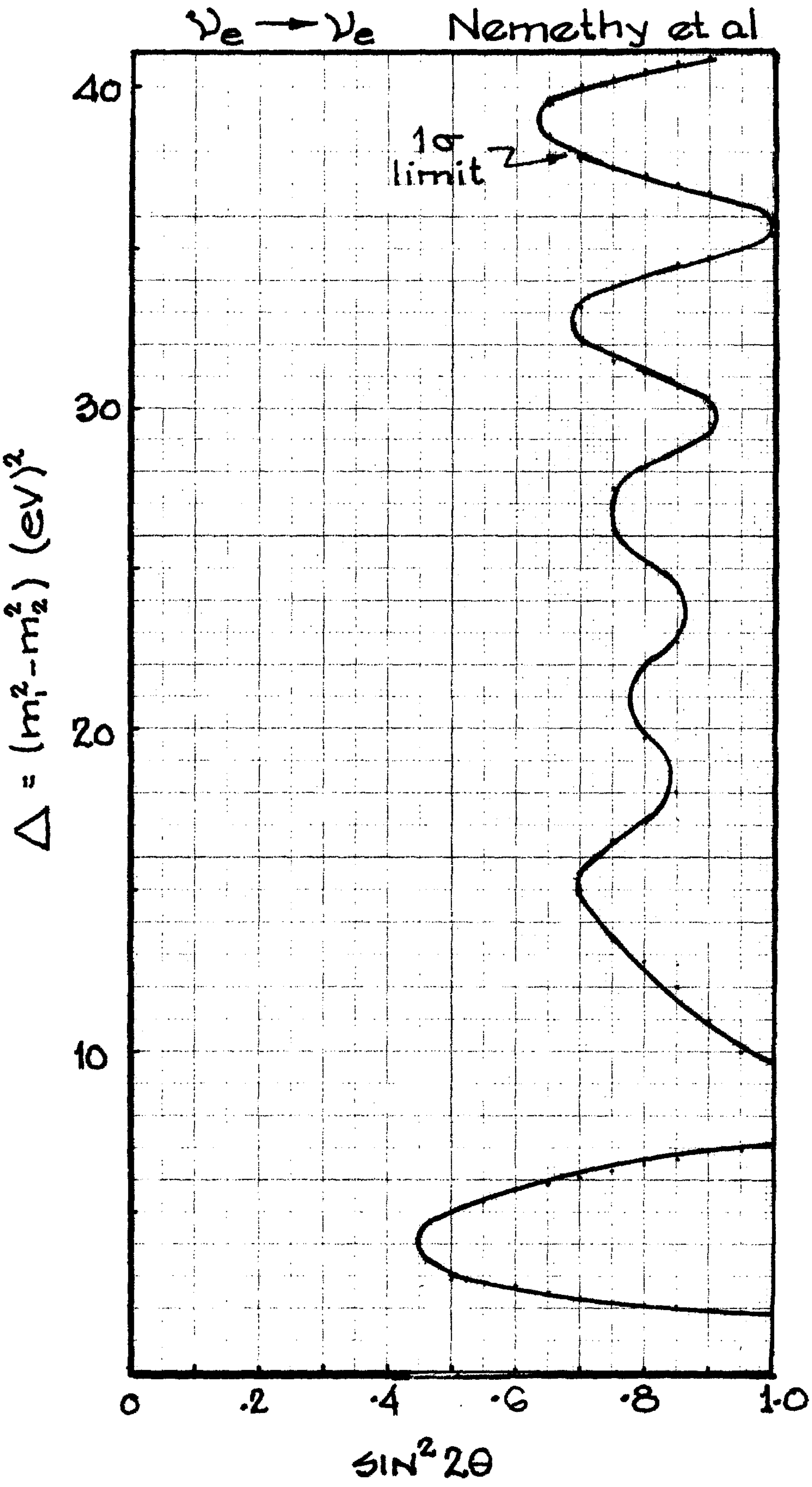

νe → νe Nemethy et al
1σ limit
Δ = (m₁² - m₂²) (eV)²
40
30
20
10
0
·2
·4
·6
·8
1·0
SIN² 2θ

Fig

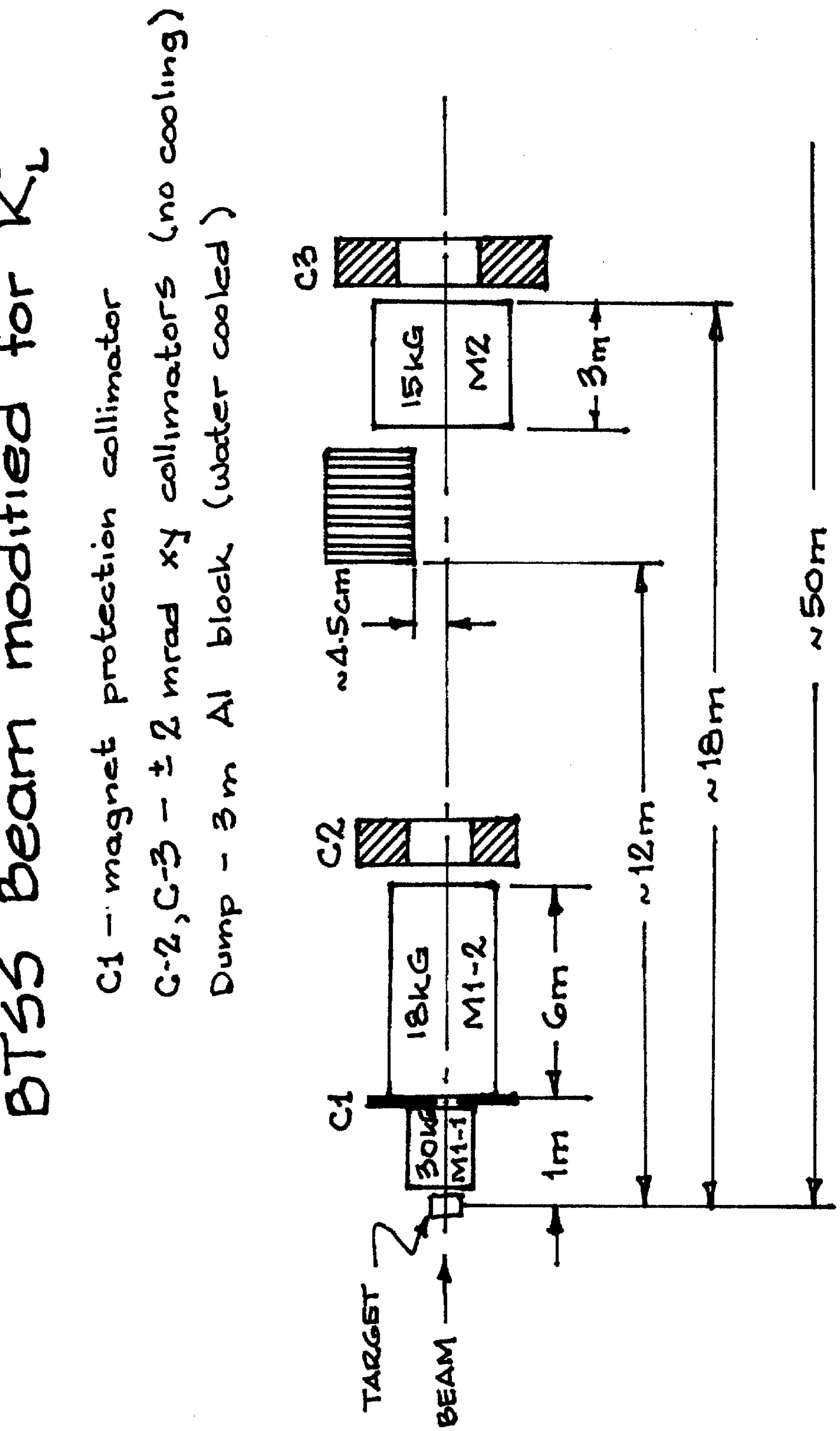

BT55 Beam modified for K^0_L
C1 – magnet protection collimator
C-2, C-3 – ± 2 mrad xy collimators (no cooling)
Dump – 3m Al block (water cooled)
TARGET
BEAM
C1
30kG
M1-1
1m
18kG
M1-2
6m
C2
~12m
~4.5cm
15kG
M2
3m
C3
~18m
~50m

FIGURE 2
3

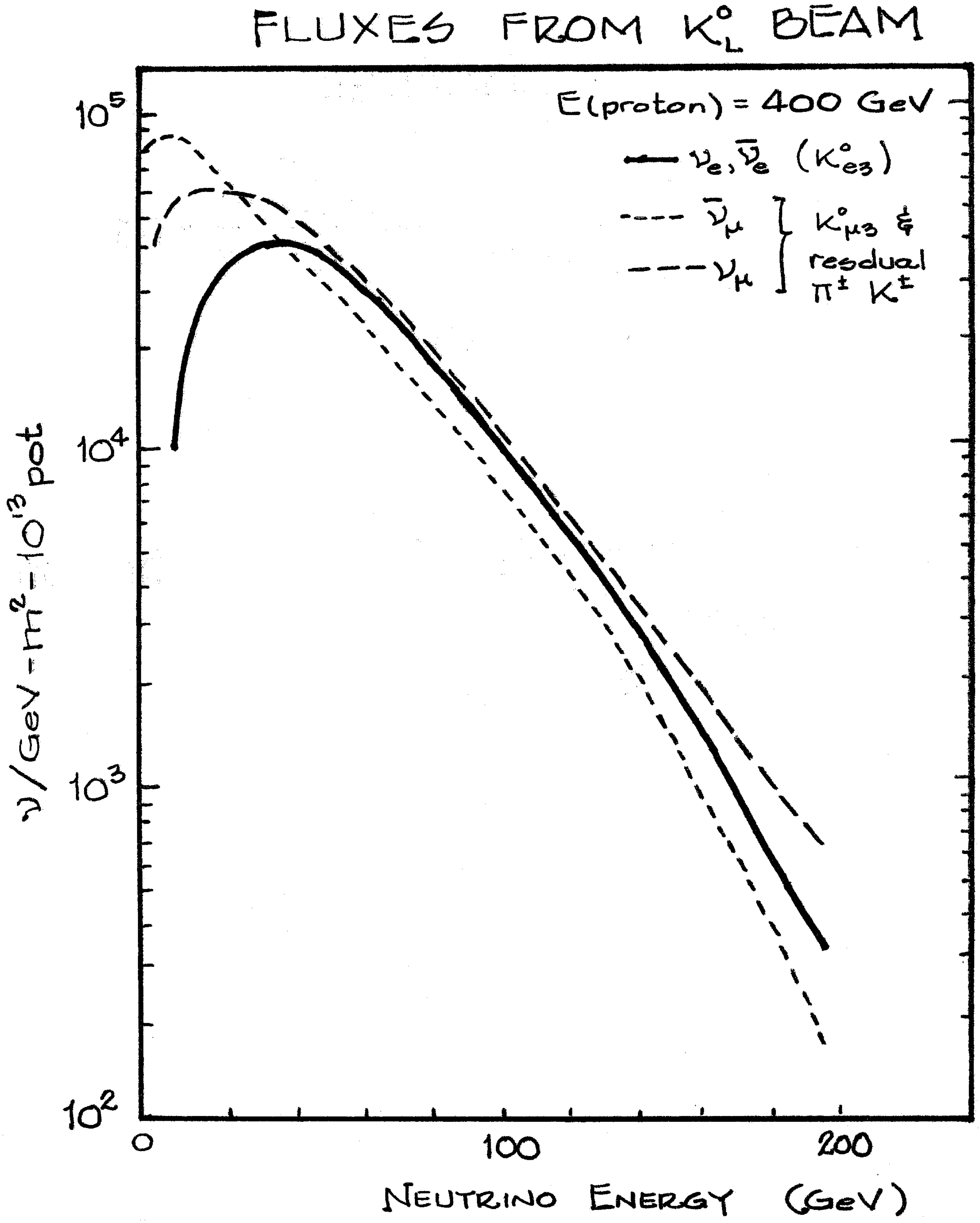
FLUXES FROM K^0_L BEAM
E(proton) = 400 GeV
$\nu_e, \bar{\nu}_e$ (K^0_{e3})
$\bar{\nu}_\mu$
ν_μ
$K^0_{\mu 3}$ & resdual $\pi^\pm$ $K^\pm$
10^5
10^4
10^3
10^2
ν/GeV - m^2 - 10^{13} pot
0
100
200
NEUTRINO ENERGY (GeV)

FIGURE 3

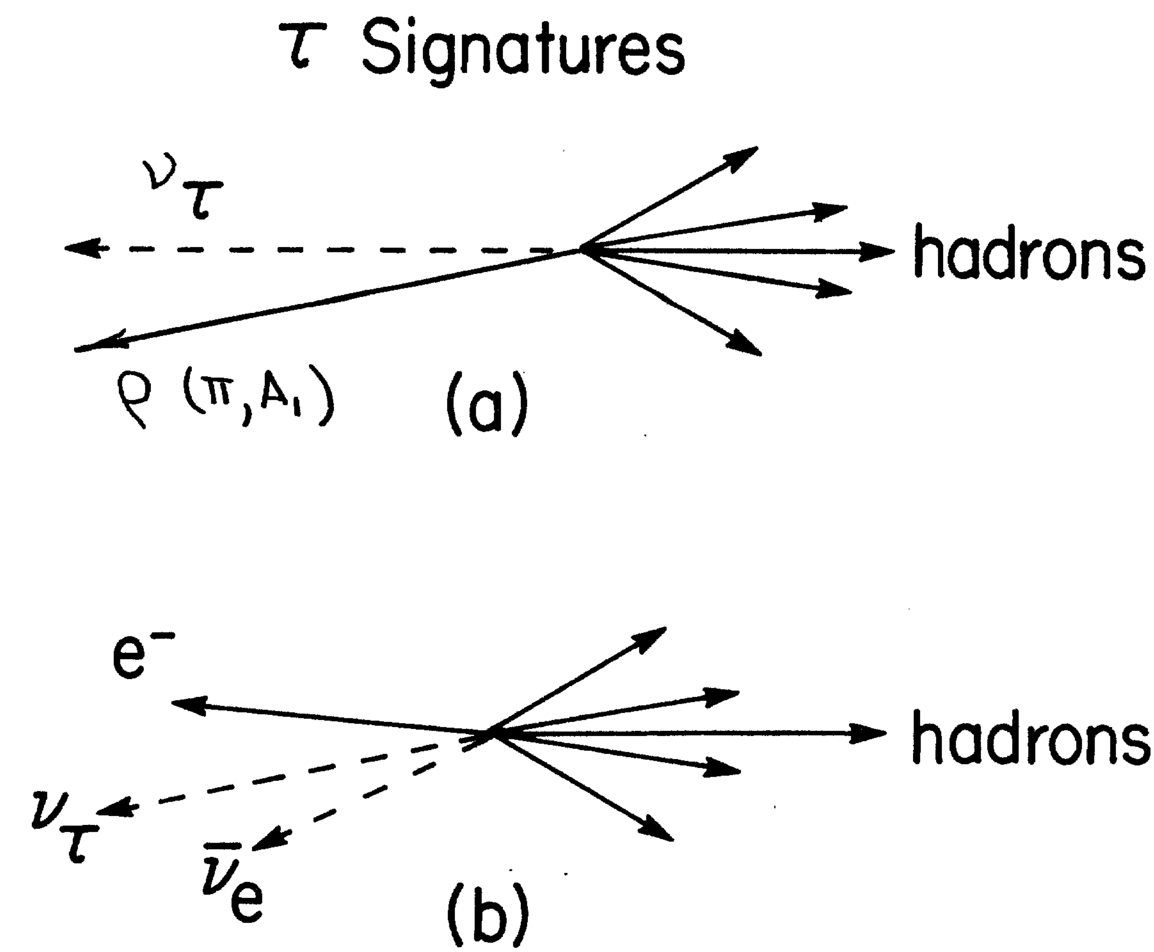

FIGURE 5

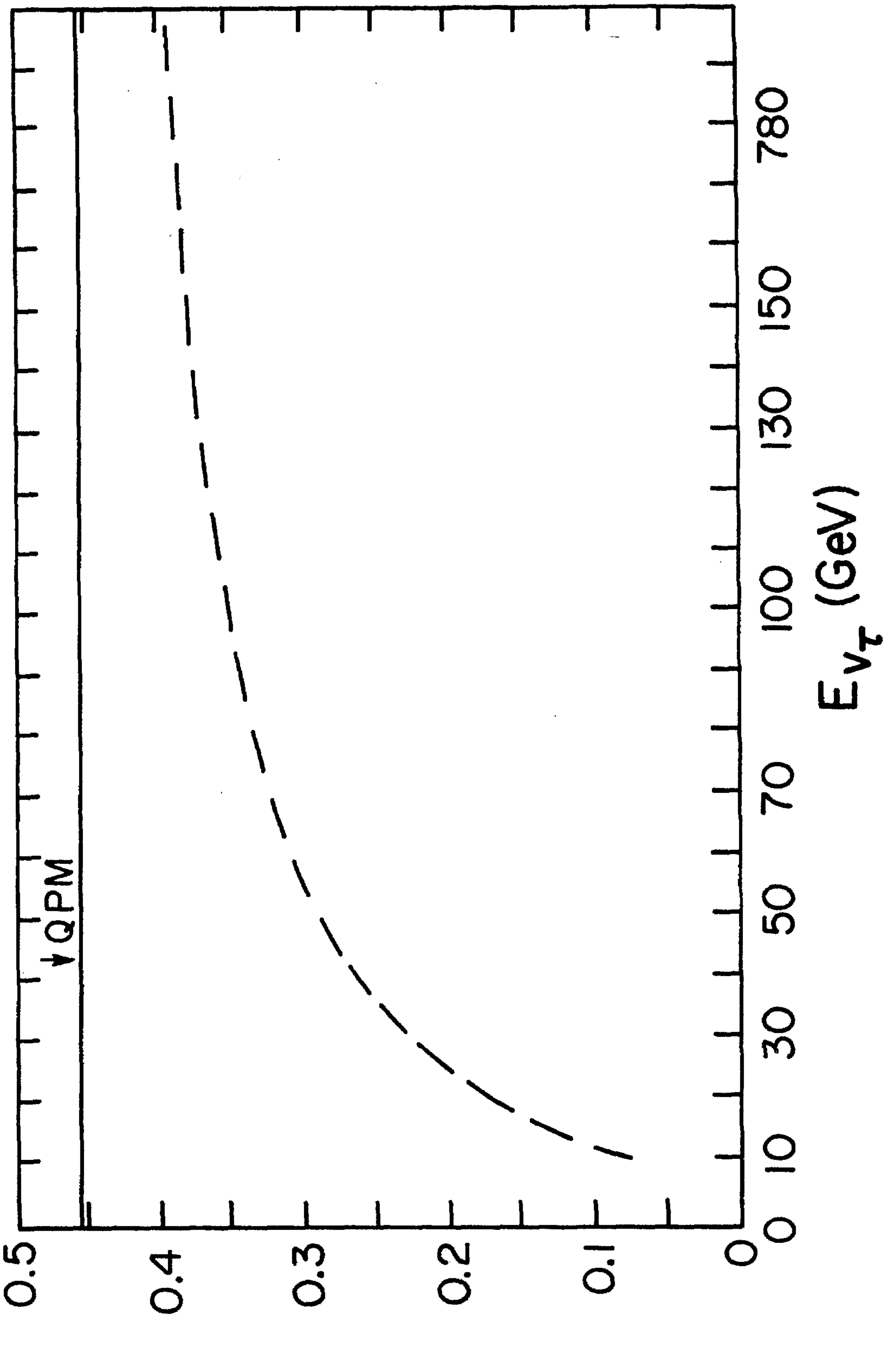

FIGURE 6

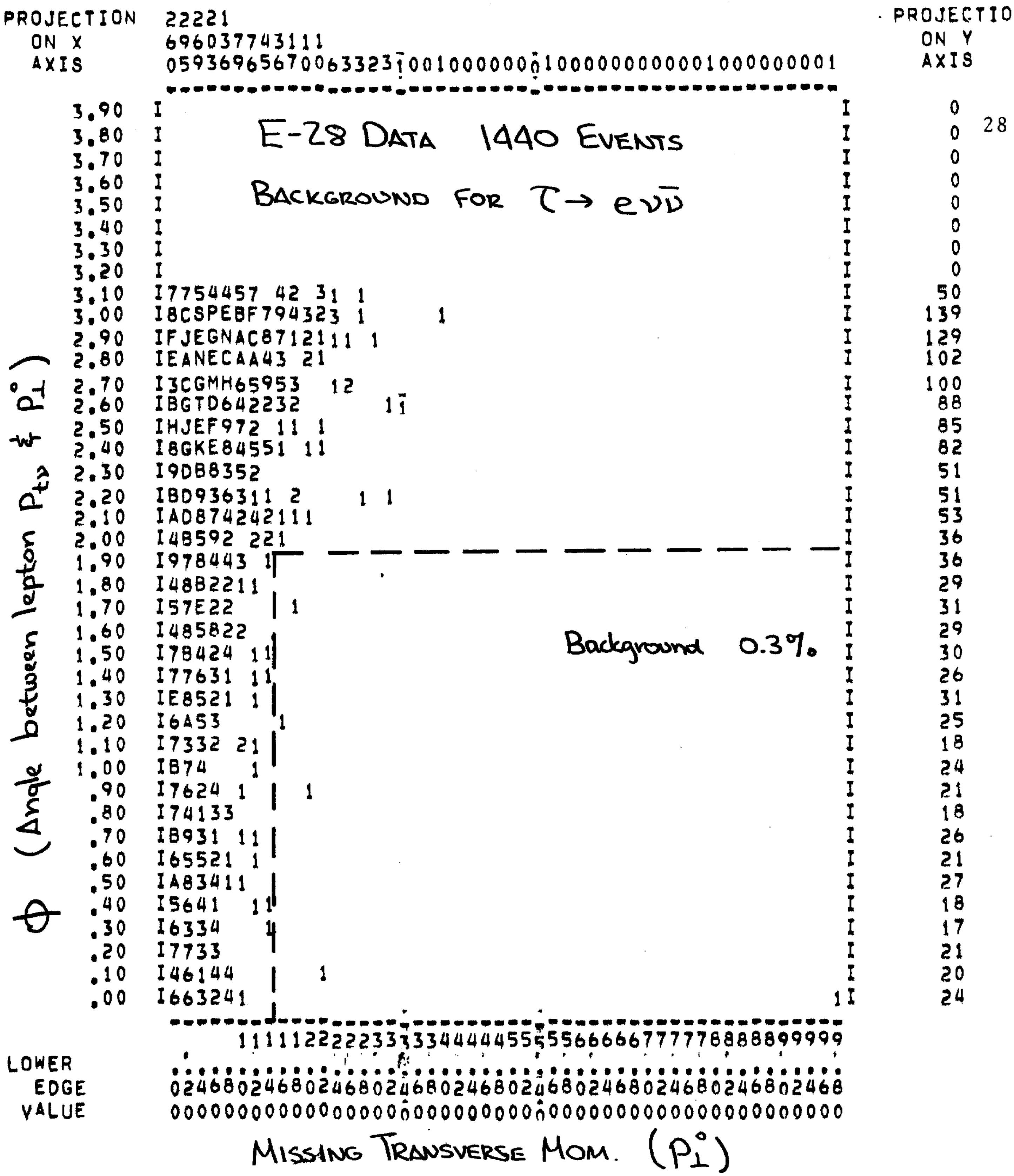
PROJECTION ON X AXIS
PROJECTION ON Y AXIS
E-28 DATA 1440 EVENTS
BACKGROUND FOR $\tau \to e\nu\bar{\nu}$
Background 0.3%
LOWER EDGE VALUE
MISSING TRANSVERSE MOM. ($P_\perp^\circ$)
Φ (Angle between lepton $P_{t\nu}$ & $P_\perp^\circ$)

FIGURE ~~6~~a 7

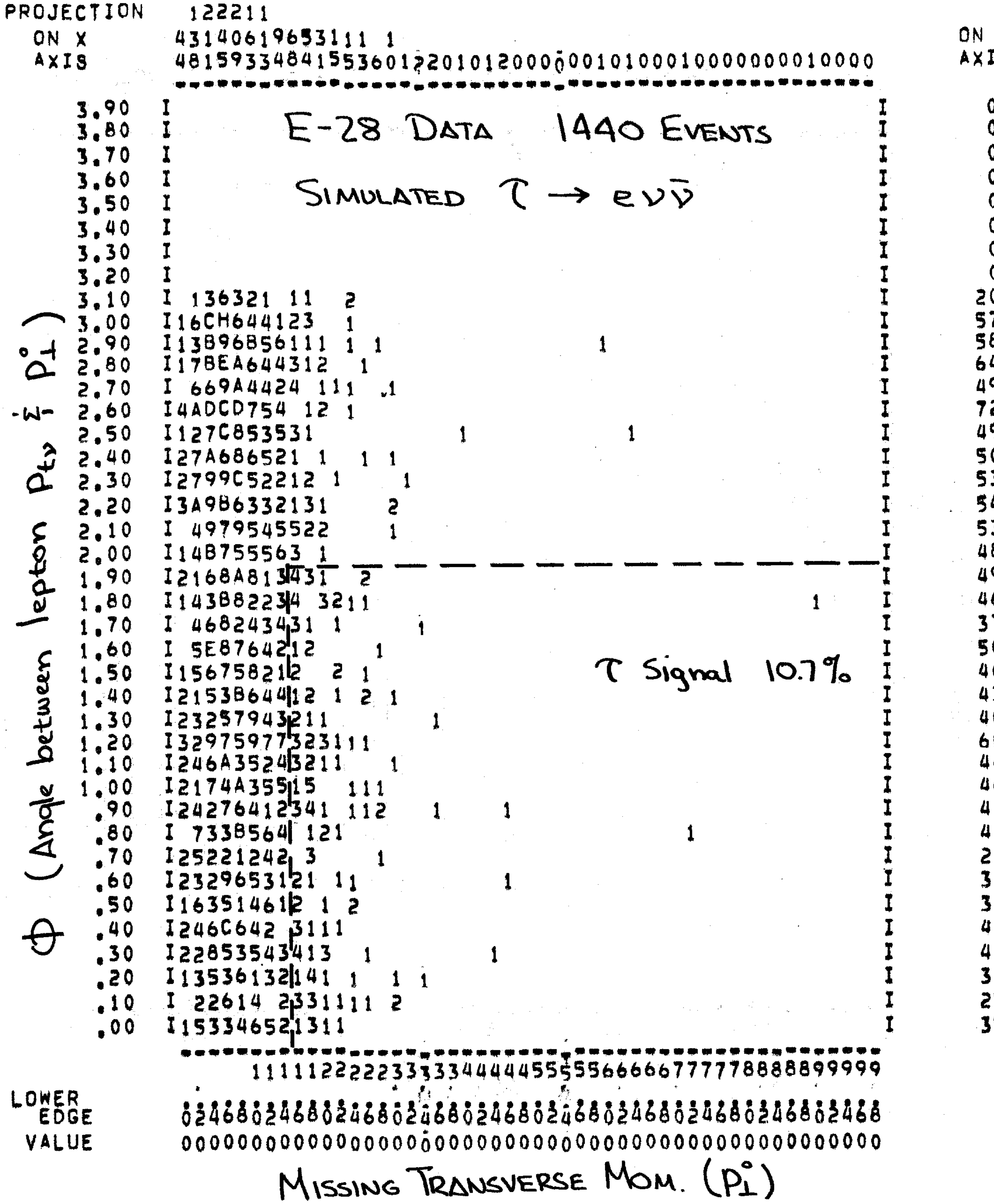
PROJECTION ON X AXIS
ON Y AXIS
E-28 DATA 1440 EVENTS
SIMULATED τ → eνν̄
τ Signal 10.7%
Φ (Angle between lepton $P_{t\nu}$ & $P_\perp^\circ$)
LOWER EDGE VALUE
MISSING TRANSVERSE MOM. ($P_\perp^\circ$)

FIGURE 7b

GAMMA-GAMMA MASS SPECTRUM

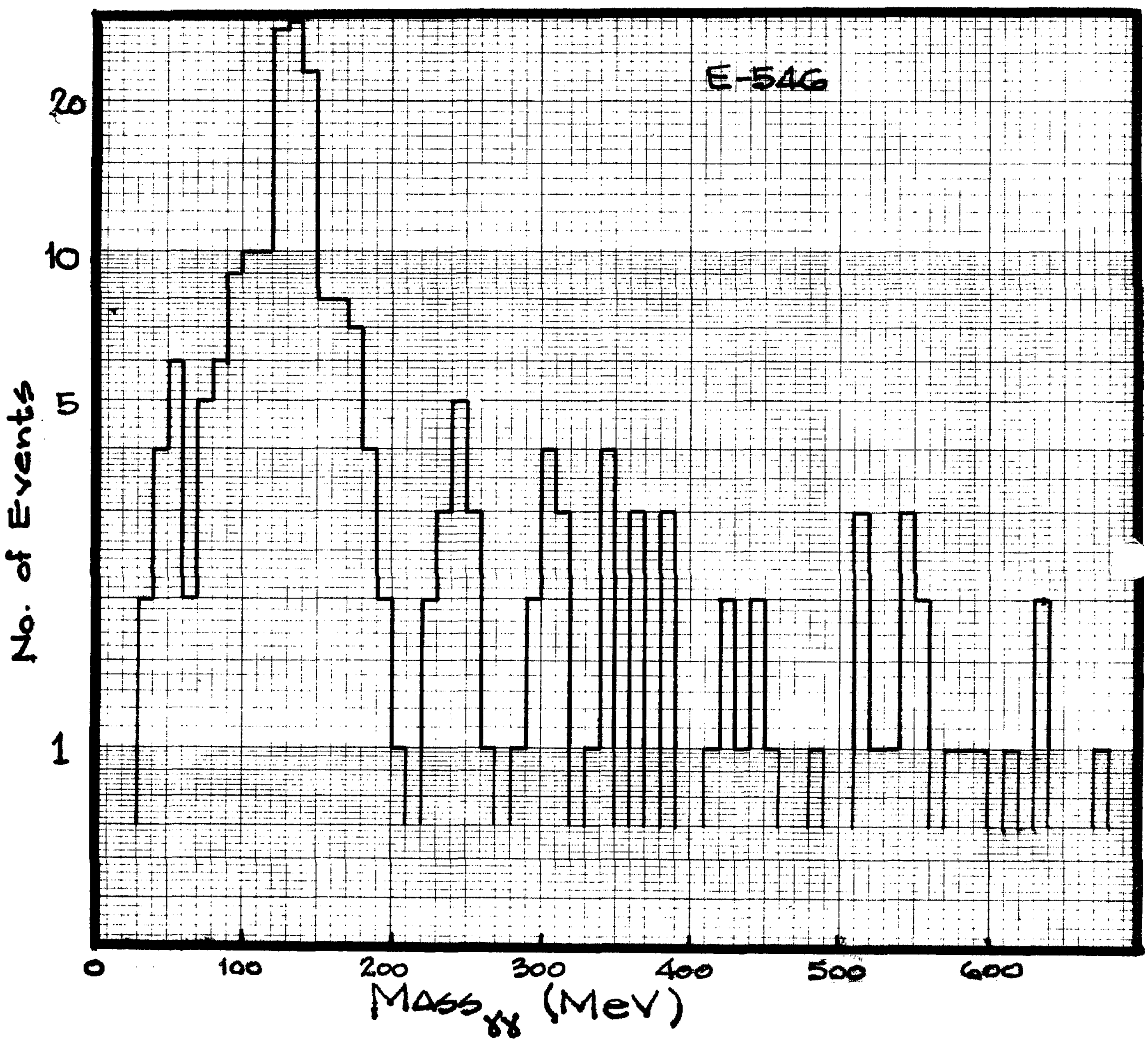

FIGURE 7 8

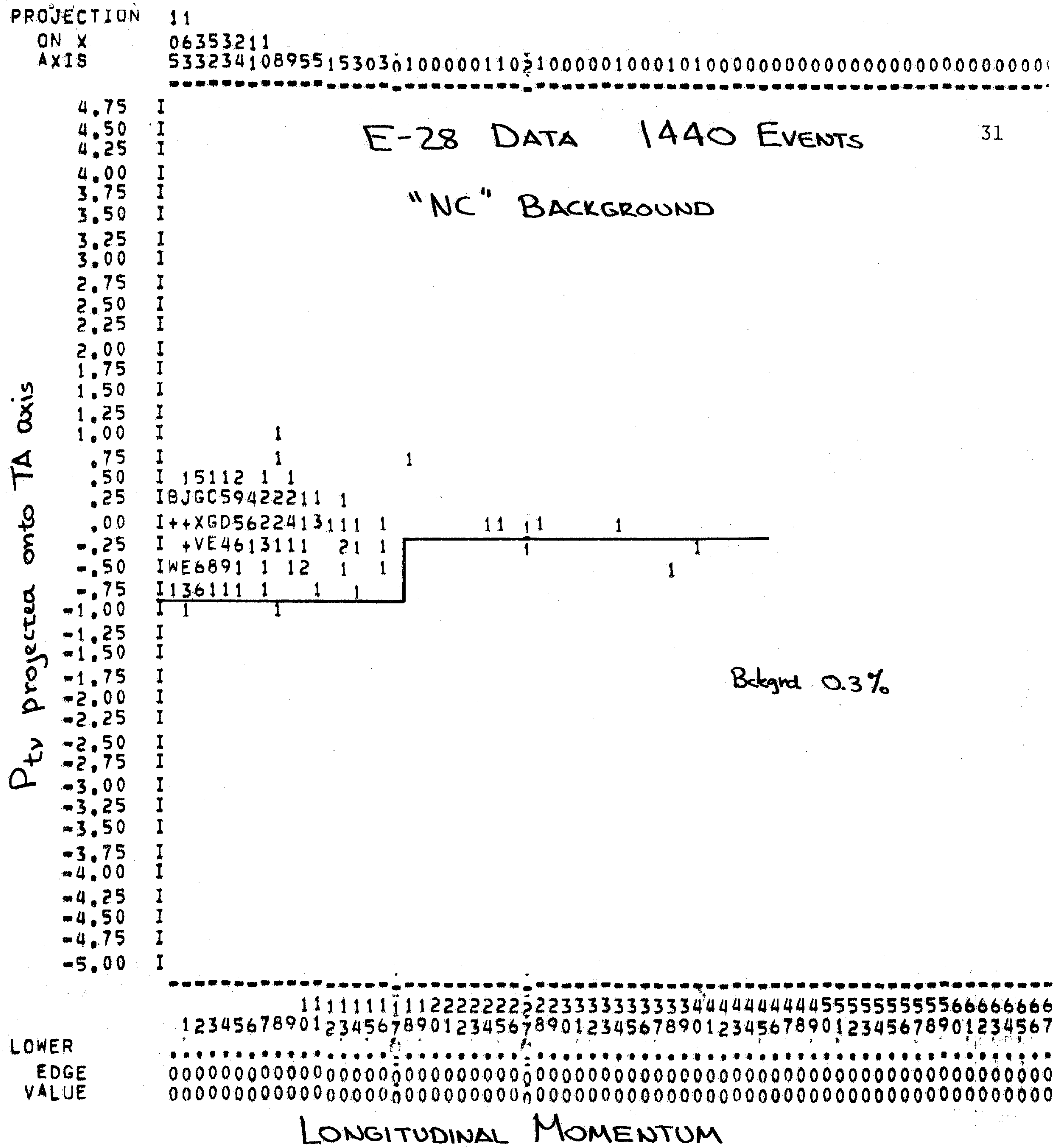
PROJECTION ON X AXIS
E-28 DATA 1440 EVENTS
"NC" BACKGROUND
Bckgrd 0.3%
Ptv projected onto TA axis
LOWER EDGE VALUE
LONGITUDINAL MOMENTUM

FIGURE 9a

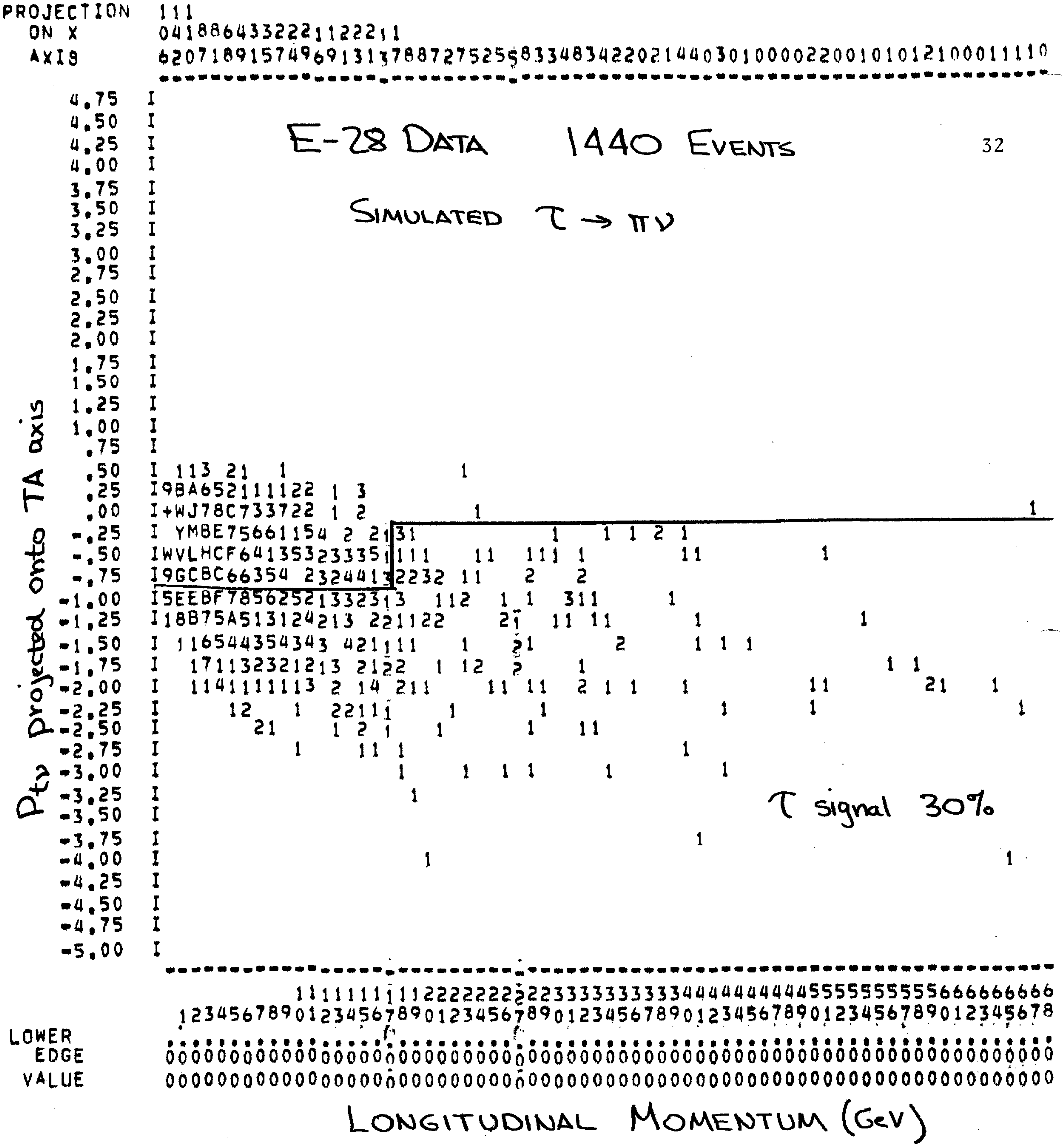
PROJECTION ON X AXIS
E-28 DATA 1440 EVENTS
SIMULATED τ → πν
τ signal 30%
Pτν projected onto TA axis
LOWER EDGE VALUE
LONGITUDINAL MOMENTUM (GeV)

FIGURE 9b

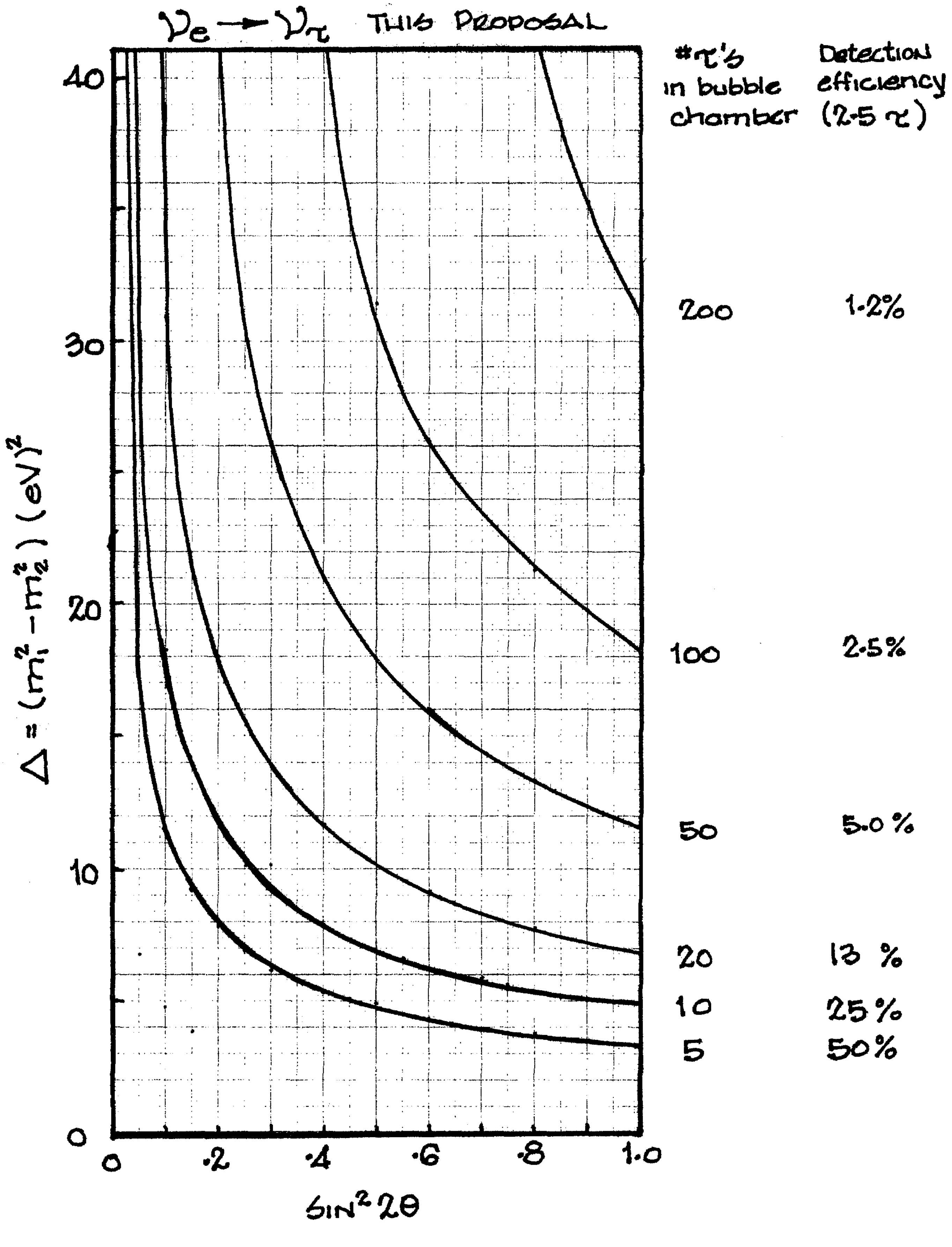

$\nu_e \rightarrow \nu_\tau$ THIS PROPOSAL
#τ's in bubble chamber
Detection efficiency (2.5 τ)
200
1.2%
100
2.5%
50
5.0%
20
13 %
10
25%
5
50%
40
30
20
10
0
·2
·4
·6
·8
1.0
$\Delta = (m_1^2 - m_2^2)\ (eV)^2$
$\sin^2 2\theta$

Fig 10

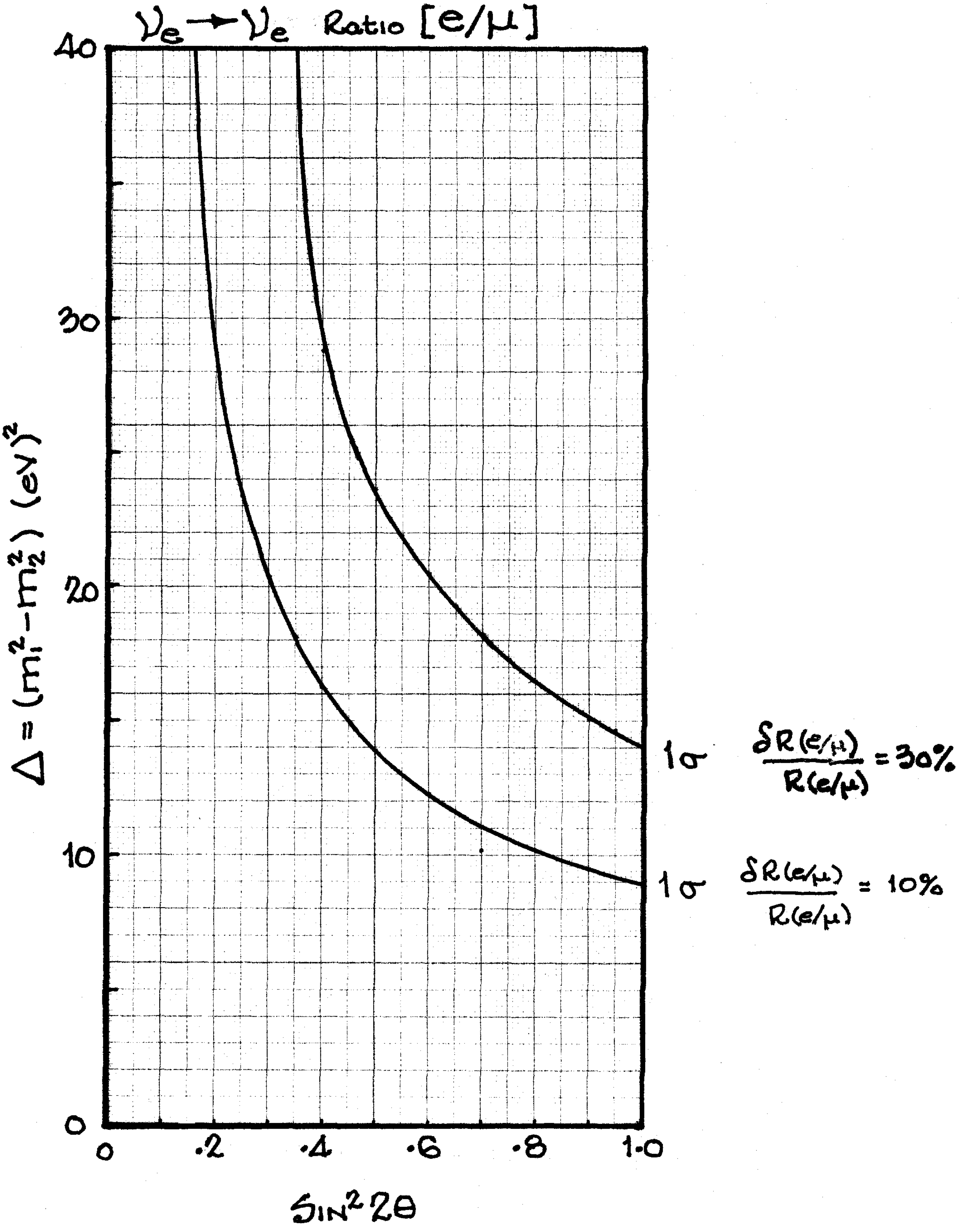

$\nu_e \rightarrow \nu_e$ Ratio [e/μ]
40
30
20
10
0
$\Delta = (m_1^2 - m_2^2)\ (eV)^2$
0
.2
.4
.6
.8
1.0
$\sin^2 2\theta$
1σ $\frac{\delta R(e/\mu)}{R(e/\mu)} = 30\%$
1σ $\frac{\delta R(e/\mu)}{R(e/\mu)} = 10\%$

Fig 11

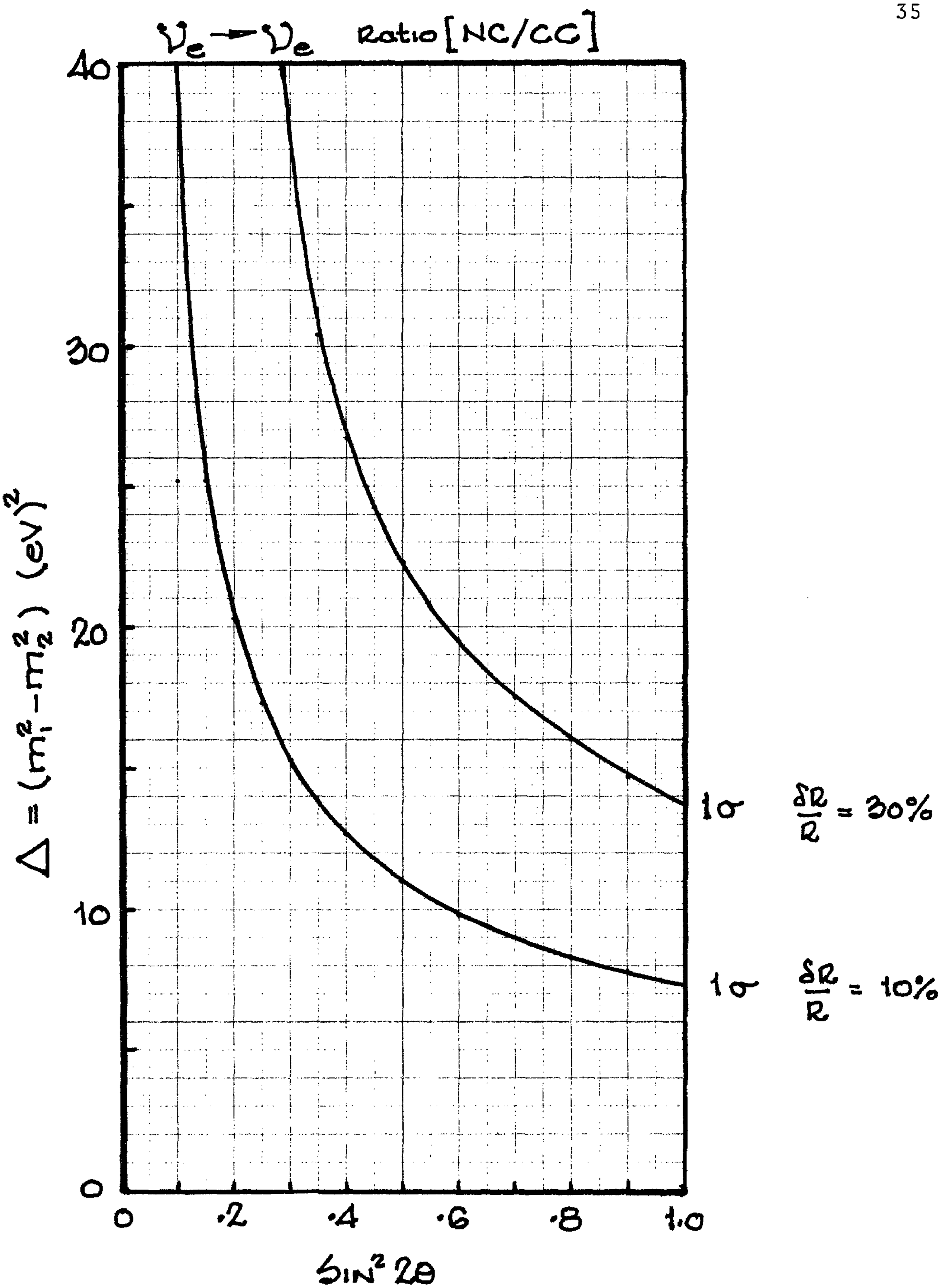
$\nu_e \to \nu_e$ Ratio [NC/CC]
40
30
20
10
0
$\Delta = (m_1^2 - m_2^2)\ (eV)^2$
0
·2
·4
·6
·8
1.0
$\sin^2 2\theta$
$1\sigma \quad \frac{\delta R}{R} = 30\%$
$1\sigma \quad \frac{\delta R}{R} = 10\%$

Fig 12